

# CFD Analysis on the Bare Hull Form of Submarines for Minimizing the Resistance

Mohammad Moonesun<sup>1,2\*</sup>, Yuri Mikhailovich Korol<sup>3</sup>, Hosein Dalayeli<sup>1</sup>

<sup>1\*</sup> Faculty of MUT, Shahin shahr, Iran; [m.moonesun@gmail.com](mailto:m.moonesun@gmail.com)

<sup>2</sup> National University of Shipbuilding Admiral Makarov (NUOS), PhD student, Ukraine

<sup>3</sup> National University of Shipbuilding Admiral Makarov (NUOS), Faculty of Ship Hydrodynamic, Professor in ship design, Ukraine

## ARTICLE INFO

### Article History:

Received: 21 Oct. 2014

Accepted: 14 Apr. 2015

Available online: 20 Jun. 2015

### Keywords:

Submarine

torpedo

hull

form

CFD

hydrodynamic

resistance

## ABSTRACT

In this paper, a CFD analysis on the bare hull form of submarines or torpedoes for minimizing the resistance is represented. There are several parameters in submarine form design which the most important parameter is resistance. All operational characteristics of submarines are related to the resistance, related required power and then, underwater speed and range. Other parameters are only mentioned. In this paper, the bare hull form is only studied without appendages. About seventy percent of the total resistance, is dedicated to the bare hull. The bare hull has three main parts: bow, cylinder and stern. The most real naval submarines and ROVs have parallel middle body form. Thus in this study, the focus is on this type of hull. The equations of bow and stern form are studied, as well. This paper, has studied the several forms by changing the coefficients of equations. CFD analyses are performed on these shapes for achieving the minimum resistance. The ratio of length on diameter (L/D) is another parameter which is studied in this paper. This analysis is conducted by Flow Vision (V.2.3) software based on CFD method and solving the RANS equations. All analyses are performed for underwater navigation, without free surface effect because, the required power is estimated always by submerged mode of navigation.

## 1. Introduction

There are some rules and concepts about submarines and submersibles shape design. There is urgent need for understanding the basis and concepts of shape design. Submarine shape design is strictly depended on the hydrodynamic characteristics such as other marine vehicles and ships. In submerged navigation, submarines are encountered with limited energy. Based on this fact, the minimum resistance is then vital in submarine hydrodynamic design. In addition, the shape design depends on the internal architecture and general arrangements of submarine. In real naval submarines, the submerged mode is the base for determination of the hull form. The several parts of submarine are bare hull and sailing. The parts of bare hull are the bow, middle part and stern. The focus of this paper is on this type of bare hull. Joubert [1, 2] describe the notes of naval submarine shape design with regarding the hydrodynamic aspects. The basis of submarine shape selection with all aspects such as general arrangement, hydrodynamic, dynamic stability, flow noise and sonar efficiency are discussed by Burcher et al. [3]. A lot of scientific material about

naval submarine hull form and appendage design with hydrodynamic considerations is presented by Yuri et al. [4]. Some studies based on CFD method about submarine hull form design with minimum resistance are done by Moonesun et al. [5-10]. Special discussions about naval submarine shape design are presented in Iranian Hydrodynamic Series of Submarines (IHSS) (Moonesun [6], IDS [11]). Some case study discussions are based on CFD method about the hydrodynamic effects of the bow shape and the overall length of the submarine are presented by Praveen et al [12] and Suman et al. [13]. Defence R&D Canada [14, 15] has suggested a hull form equation for the bare hull, sailing and appendages in the name of "DREA standard model". Alemayehu et al [16], Minnick [17] and Grant [18] present an equation for teardrop hull form with some of their limitation on coefficients but the main source of their equation is presented by Jackson [19]. The simulation of the hull form with different coefficients is performed by Stenars [20]. Another equation for torpedo hull shape is presented by Prestero [21]. Formula "Myring" as a famous formula for axis-

symmetric shapes is presented by Myring [22]. Extensive experimental results about hydrodynamic optimization of teardrop or similar shapes are presented by Hoerner [23]. This reference is known as the main reference book in the field of the selection of aerodynamic and hydrodynamic shapes based on experimental tests. Collective experimental studies about the shape design of bow and stern of the underwater vehicles that are based on the underwater missiles are presented by Greiner [24]. The most parts of this book are useful in the field of naval submarine shape design. Other experimental studies on the several teardrop shapes of submarines are presented by Denpol [25]. All equations of hull form, sailing and appendages for SUBOFF project with experimental and CFD results are presented by Groves et al [26] and Roddy [27].

## 2. Some important factors in bare hull form design

Bare hull is an outer hydrodynamic shape that envelopes the pressure hull. For a well judgment and the best selection of bare hull form, the most important factors in bare hull form design are counted as: 1) minimum submerged resistance: the fineness ratio (L/D) and the bow and stern shape are the important factors. Jerome et al [28] and Brenden [29] have studied the optimization of submarine shape according to a logical algorithm based on minimum resistance. Optimization of shape based on minimum resistance in snorkel depth is studied by Volker [30]. 2) general arrangement demands. 3) enough volume for providing enough buoyancy according to the given weight. 4) minimum flow noise specially around the sonar and acoustic sensors. 5) minimum cavitation around the propeller.

Resistance and volume are two main parameters that affect the submarine shape design. The coefficient that can describe both parameters is "Semnan" coefficient that is defined as follows:

$$\text{Semnan coefficient (Ksn)} = \frac{(\text{Volume})^{\frac{1}{3}}}{\text{Resistance Coefficient}} \quad (1)$$

Semnan coefficient can be named "Hydro-Volume efficiency". For selecting a good shape form of submarine, this coefficient is a very important parameter because it counts both resistance and volume. Larger values of this coefficient provide better design. In some cases, a shape has minimum resistance but has a little volume in a given constant length. Thus it can't be a good design.

## 3. CFD Method of Study and validation

In this article, all CFD analyses are performed by Flow Vision (V.2.3) software, which is based on CFD method and solving the RANS equations. Generally,

the validity of the results of this software has been done by several experimental test cases and nowadays, this software is accepted as a practicable and reliable software in CFD activities. In this paper, Finite Volume Method (FVM) is used for modeling the selected cases. A structured mesh with cubic cell has been used for mapping the space around the submarine. For modeling the boundary layer near the solid surfaces, the selected cells near the object are fine and very small compared to the other parts of domain. For selecting the proper number of the cells in each part of domain, an investigation is performed for a certain model. For example, seven different amount of meshes corresponding to  $nf=1.35$ ,  $na=1.35$  and  $v=10\text{m/s}$  were selected and the results were compared insofar as the results remained almost constant after 1.1 million meshes, and it shows that the results are independent of mesh size (Figure1). In all models, the mesh numbers are considered more than 1.2 millions.

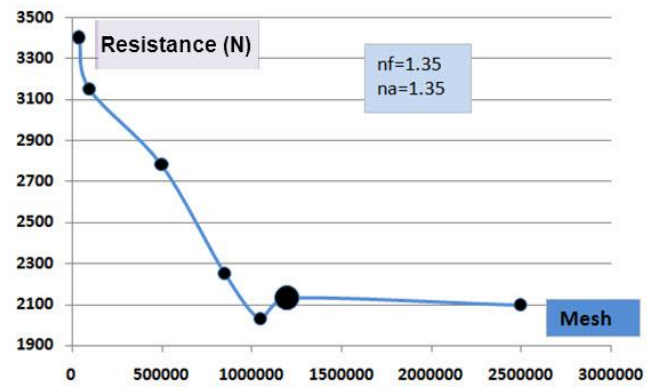


Figure 1. Mesh independency evaluations

For a suitable convergence, the iteration process is continued until the tolerance of convergence (less than one percent) is satisfied. All iterations are continued to more than one million iterations. The following characteristics are used in this domain: inlet with a uniform flow, free outlet, symmetry in the four faces of the box and wall for the body of submarine. The dimensions of cubic domain for this sample case are as follows: length = 49 m (equal to 7L), beam = 7 m (equal to L or 7D) and height = 7 m (equal to L or 7D). Due to the axis-symmetry only a quarter of the body needs to be modeled, requiring very few computation time. Meanwhile, this study has shown that the beam and height equal to 7D can be acceptable in this consideration. Here there is no need for fine meshes far away from the object. The forward distance of the model is equal to 2L and after distance is 4L in the total length of 7L (Figure2). In each part of this paper, the dimensions of model and domain are different. The turbulence model is K-epsilon and  $y^+$  is considered equal to 30. The considered flow is incompressible fluid flow (fresh water) at 20 degrees centigrade and a constant velocity of 10 m/s. The results have been validated by experimental results [12]. In this reference, there are experimental

and empirical results for several submarine bare hull forms. For validating the CFD results, the models of C and E of this reference are analyzed.

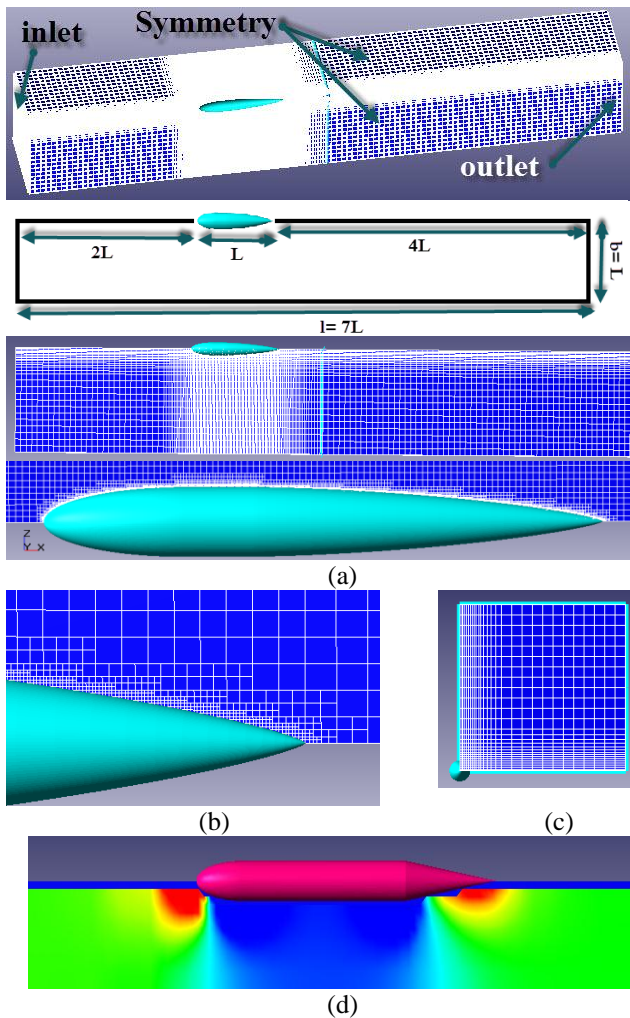


Figure 2. (a) Domain and structured grid (b) Very tiny cells near the wall for boundary layer modeling and keeping  $y^+$  about 30 (c) Quarterly modeling because of axis-symmetry (d) pressure field around the body

The specifications of these models are presented by Praveen [12]. The comparison of the results is performed in Table 1. It shows the difference less than five percent with experimental results. Empirical results which are based on Empirical formula are not so accurate, and is suitable for general estimation only.

Table 1. The comparison of  $X^*10000$  values in several methods [12]

Models	Empirical	experimental	CFD	Difference (%)
Model C	6.9	7.85	8.05	2.5
Model E	5.7	6.22	6.43	3.4

#### 4. General samples in submarine hull form design

There are six models with torpedo shape without any appendages. According to Figure3, all proposed models are identical in length (equal to 10 meters), diameter (equal to 2 meters) and fineness ratio  $L/D$  (equal to 5), but contain different volumes. In all

models, bow length is equal to 2 meters, and stern length is 3 meters. Middle part is a cylinder with a length of 5 meters. Model 1 is a simple cylinder without a tapered bow and stern. This model shows the most resistance coefficient and the worst selection. Model 2 is a cylinder, but with a conical stern. Model 3 is a cylinder, but with an elliptical bow. Model 4 has a conical bow and stern. Model 5 has an elliptical bow and conical stern such as today's submarines. Model 6 is similar to Model 5 but with a curved stern instead of the conical stern. This curvature is provided by a sector of a circle with radius of 5 meters. This sector is tangent to the cylinder without any discontinuity.

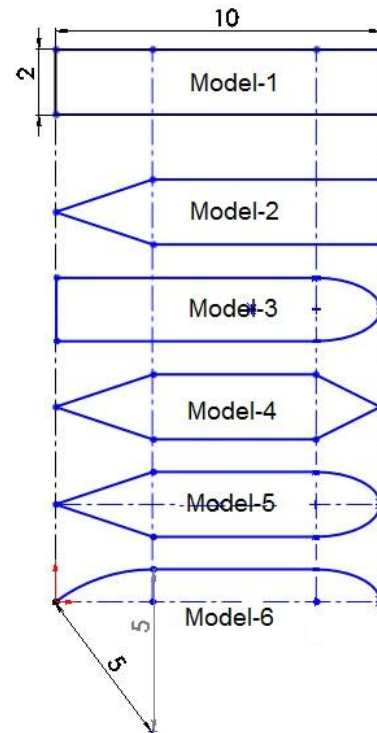


Figure 3. Shapes of six models

The total resistance is equal to the summation of frictional and pressure resistance. For all six models, the total resistance coefficient versus Reynolds number diagrams are shown in Figure 4. All resistance coefficients are based on the cross section area equal to 3.14 square meters. Logically, the first model has the most resistance coefficient and the sixth model in this regard tends to have the minimum value. However, the amount of difference between the models is important and considerable. Focusing attention on these differences can show the logic of submarine shape design. From obtained results, some questions in these fields can now be answered. For example: Why can the sharp shape not be used for submarines?, Why should the stern be conical?, Why should the bow be curved?, Why is the curved stern better than the simple conical stern?, and so on. The pressure resistance coefficient versus Reynolds number diagrams are shown in Figure5. The pressure resistance is a function of the shape of the object (submarine) and, based on this fact, it is named "form

resistance". All coefficients after Reynolds of 5 million are almost constant.

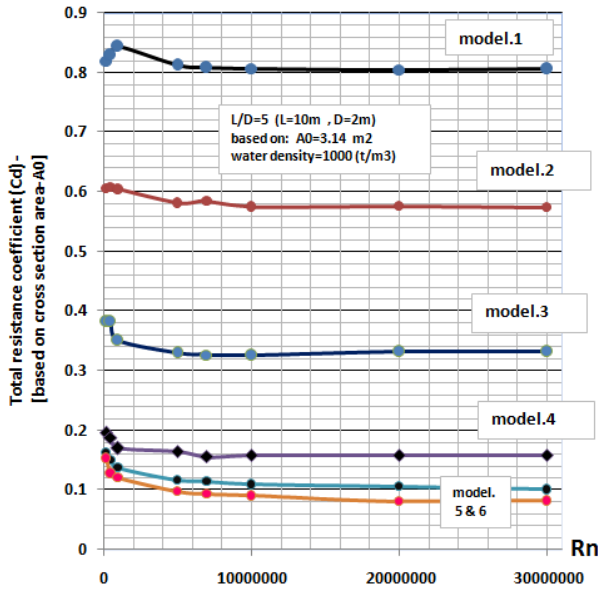


Figure 4. variation of the total resistance coefficient versus Reynolds number for six models

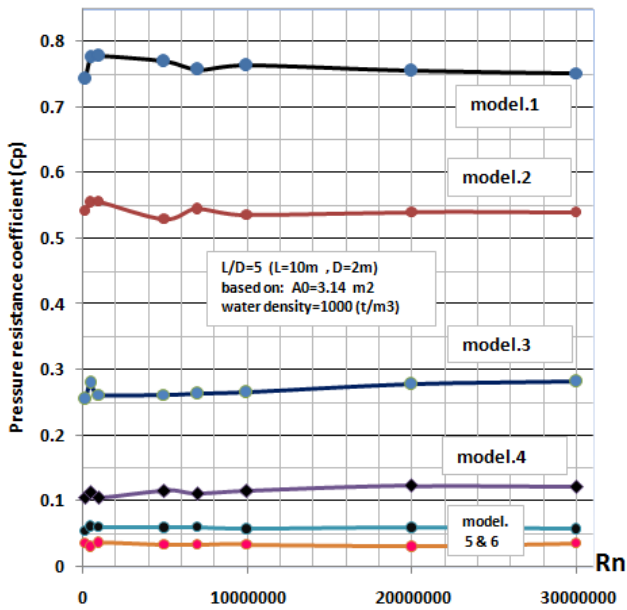


Figure 5. variation of the pressure resistance coefficient versus Reynolds number for six models

It can be concluded that: 1- Bow and stern of submarine should be tapered gradually (by comparison between models 1 and the other models). 2- Sharp narrow bow isn't a good selection, but a blunt shape such as an elliptical bow is recommended (by comparison between models 4 and 5). 3- Curved stern is better than conical stern (by comparison between models 5 and 6). 4- Effects of the bow on the resistance are strongly more than the effects of the stern (by comparison between models 2 and 4). 5- Curved bow (such as elliptical) and curved stern (such as a sector of circle or parabolic) with cylindrical middle part can be a good recommendation for submarines and submersibles (by comparison between model 6 and the other models).

## 5. Bare hull form design

### 5.1. Bare hull form equations

The equations of bare hull are presented as "Hull Envelope Equation" [16-20]. The envelope is first developed as a pure tear drop shape with the forward body, comprising 40 percent of the length, and the after body comprising the remaining 60 percent [18]. The forward body is generated by revolving an ellipse about its major axis and is described by the following equation:

$$Y_f = R \left[ 1 - \left( \frac{X_f}{L_f} \right)^{n_f} \right]^{1/n_f} \quad (2)$$

The after body is generated by revolving a line around axis and is described by:

$$Y_a = R \left[ 1 - \left( \frac{X_a}{L_a} \right)^{n_a} \right] \quad (3)$$

The quantities  $Y_a$  and  $Y_f$  are the local radius of the respective body of revolution with  $X_a$  and  $X_f$  describing the local position of the radius along the body (Figure 6). If a parallel middle body is added to the envelope, then the cylindrical section with a radius equal to the maximum radius of the fore and after body is inserted in between them. The local radii represent the offsets for drawing the submarine hull and also determine the prismatic coefficient for the hull section. The prismatic coefficient ( $C_p$ ) is a hull form parameter for fullness and is expressed as a ratio of volume of body of revolution divided by the volume of a right cylinder with the same maximum radius. For an optimum shape, the fore and after bodies will have different values for  $C_p$ . The  $C_p$  ratio is used to determine the total hull volume. The total hull volume is obtained by the following relation:

$$\text{Volume} = \frac{\pi D^2}{4} \left[ 3.6 D C_{pa} + \left( \frac{L}{D} - 6 \right) D + 2.4 D C_{pf} \right] \quad (4)$$

Where the added term,  $\left( \frac{L}{D} - 6 \right) D$ , accounts for the volume of the parallel middle body with  $C_p=1$ . The surface area of the body can be described by the following relation:

$$\text{Wetted Surface} = \pi D^2 \left[ 3.6 D C_{sa} + \left( \frac{L}{D} - 6 \right) D + 2.4 D C_{sf} \right] \quad (5)$$

Surface coefficient,  $C_s$ , describes the ratio of the surface area of the body to the surface area of a cylinder with the same maximum radius. The factors  $n_f$  and  $n_a$  appearing in the equations describe the "fullness" of the body by affecting the curvature of the parabolas. The ranges of some important parameters,



in relation to a sample case, are reported in Figure 7. The considered equations are presented in another form with regard to the other coordinate system as shown in Figure 8 [17, 29, 30].

$$r_a = R \left( 1 - \left( \frac{L_a - x}{L_a} \right)^{n_a} \right) \quad (6)$$

$$r_f = R \left( 1 - \left( \frac{(x - L_a - L_c)}{L_f} \right)^{n_f} \right)^{1/n_f} \quad (7)$$

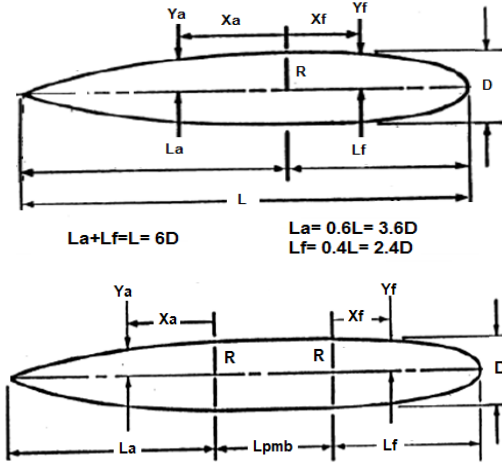


Figure 6. Parameters and coordinate system for submarine hull [16]

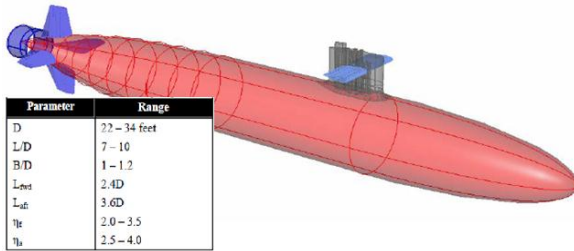


Figure 7. A sample case of hull form according to power series form with values of na and nf[20]

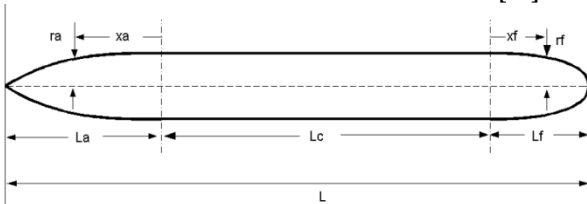


Figure 8. parameters and coordinate system for submarine hull

Other famous equations are the equations of "DREA Model" that is shown in Figure 9 and includes the specification of the bare hull and appendages.

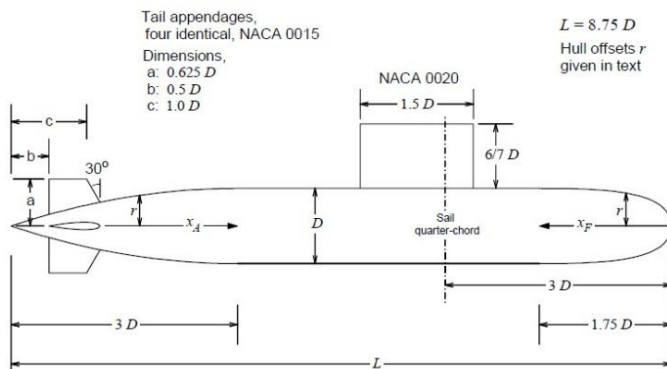


Figure 9. Parameters of DREA submarine hull [14]

The DREA model is specified in three sections; bow, mid body and tail. The fineness ratio (L/D) is equal to 8.75 so that the bow length is equal to 1.75D, the mid body length is 4D and the stern length is 3D. The axis-symmetric profile of the bow is determined by the following equation:

$$\frac{r}{D} = 0.8685 \sqrt{\frac{x_F}{D}} - 0.3978 \frac{x_F}{D} + 0.006511 \left( \frac{x_F}{D} \right)^2 + 0.005086 \left( \frac{x_F}{D} \right)^3 \quad (8)$$

The axis-symmetric parabolic profile of the stern is determined by the following equation:

$$\frac{r}{D} = \frac{1}{3} \left( \frac{x_A}{D} \right) - \frac{1}{18} \left( \frac{x_A}{D} \right)^2 \quad (9)$$

## 5.2. Specifications of the Models

In each model the bow and stern form is changed by the coefficients "nf" and "na". The middle part is a cylinder. In this section, 11 models are studied. The 3D models and their properties are modeled in SolidWorks (Figure 10). For evaluating the hydrodynamic effects of the bare hull, the lengths of stern, middle and bow and the total length are assumed to be constant. The fineness ratio (L/D) is constant as well, because the maximum diameter is constant. Therefore, the models have different volumes and wetted surface areas. The main assumptions are reported in Table 2. The specifications of all 11 models are presented in Table 3.

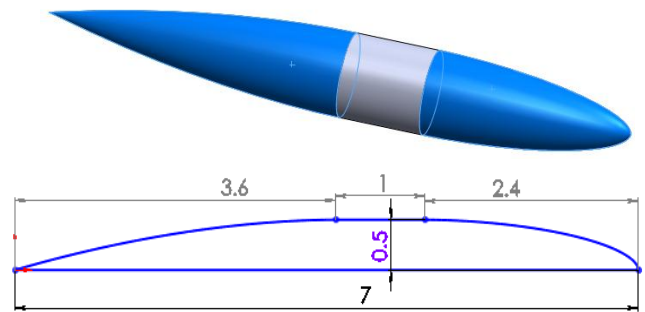


Figure 10. General configuration of the models

Table 2. Main assumptions of the models

v (m/s)	L <sub>t</sub> (m)	L <sub>f</sub> (m)	L <sub>m</sub> (m)	L <sub>a</sub> (m)	D (m)	L <sub>t</sub> /D	A <sub>0</sub> (m <sup>2</sup> )
10	7	2.4	1	3.6	1	7	3.14

Table 3. Specifications of the models

Model	specification of Model	Aw	V
1	nf=1.35, na=1.35	14.6	2.89
2	nf=1.35, na=1.85	15.45	3.15
3	nf=1.35, na=4	17.18	3.71
4	nf=1.5, na=1.5	15.22	3.07
5	nf=1.85, na=1.85	16.37	3.43
6	nf=2, na=2	16.57	3.49
7	nf=2.5, na=2.75	18.03	3.96
8	nf=3, na=3	18.55	4.13
9	nf=3.5, na=3.5	19.1	4.31
10	nf=4, na=2.75	18.76	4.19
11	nf=4, na=4	19.53	4.44

The wetted surface area ( $A_w$ ) is used for the resistance coefficient and the total volume is used for "Semnan" coefficient. In this study, the velocity is so selected that the Reynolds number could be more than five millions. It is because that, according to Ref.[10], in instances where the Reynolds number is more than five millions the total resistance coefficient remains unchanged. All configurations of the models are shown in Figure11.

Each model has its own  $n_f$  and  $n_a$  coefficients. As shown in Figure11, the bow form varies with the coefficient  $n_f$  and the stern form varies with the coefficient  $n_a$ .

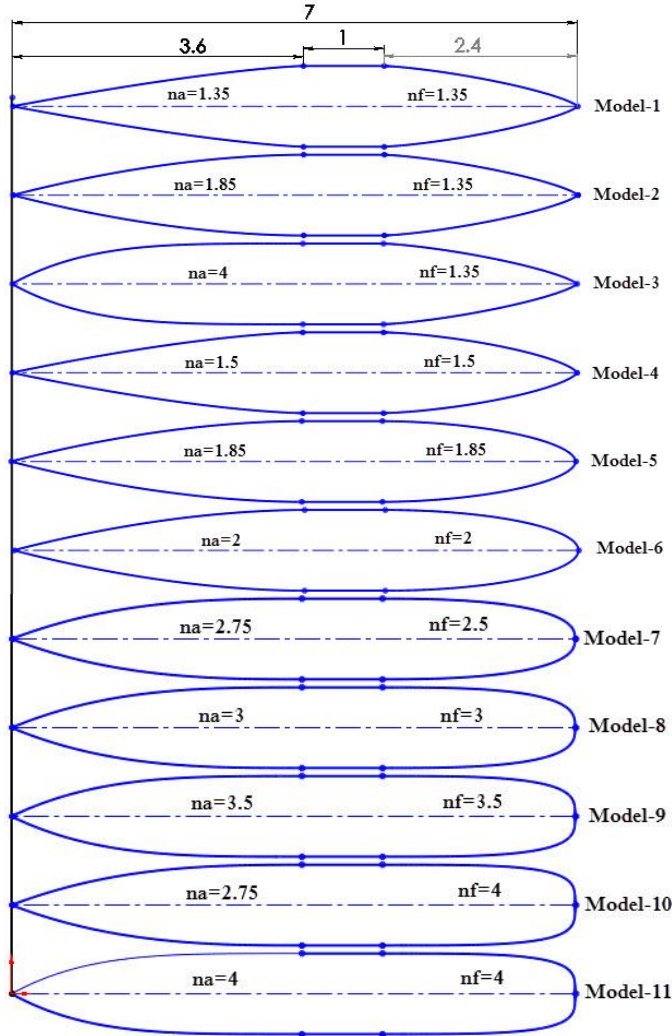


Figure 11. Configurations of the models

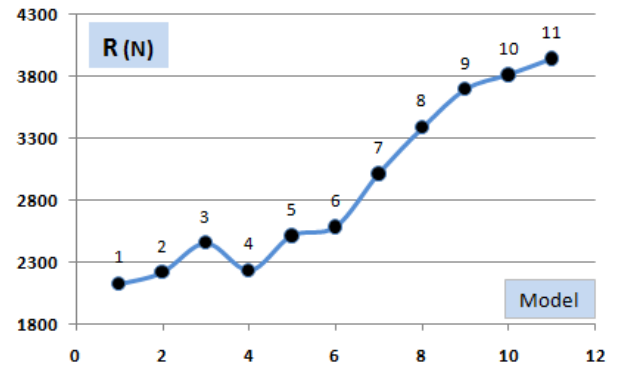
### 5.3. CFD Results Analysis

The results of analyses are reported in Table 4 and displayed in Figure 12. According to the obtained results, total resistance increases with increase in fullness of the body and coefficients of  $n_f$  and  $n_a$ . The resistance coefficient diagram based on wetted area surface similar to the total resistance diagram shows an upward trend with increasing the model number, but a (local) minimum value occurs for model 3, with  $n_f=1.35$  and  $n_a=4$ . It means that, under the assumption of constant wetted surface area, the bare hull form with  $n_f=1.35$  and  $n_a=4$  provides the

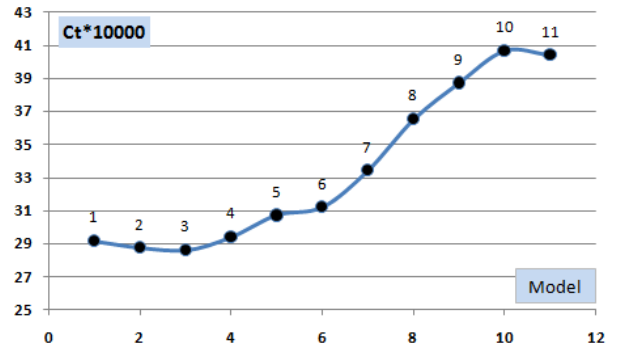
Table 4. Total resistance, resistance coefficient (based on wetted area surface ) and Semnan coefficient of the models

Model	R	Ct*10000	Semnan Coef./10
1	2128	29.15	48.85
2	2220	28.74	50.99
3	2456	28.59	54.12
4	2236	29.38	49.45
5	2512	30.69	49.12
6	2584	31.19	48.61
7	3012	33.41	47.33
8	3388	36.53	43.90
9	3696	38.70	42.03
10	3812	40.64	39.65
11	3944	40.39	40.67

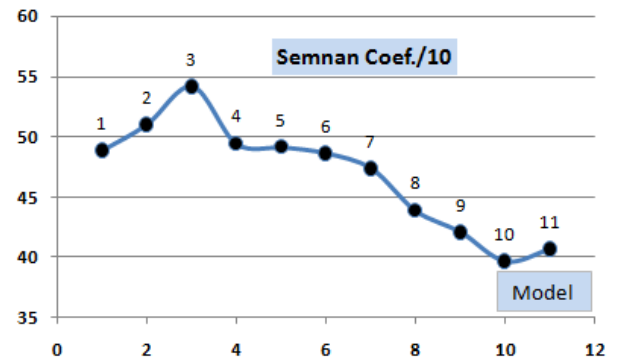
minimum value of the resistance and, hence, it is the best result. For selecting a good shape form for a submarine, enough volume should be provided; thus Semnan coefficient is a very important coefficient and should be regarded.



(a) Total resistance for each Model



(b) Total resistance coefficient for each Model (based on wetted area surface )



(c) Semnan coefficient for each Model

Figure 12. Specifications of Models with different forms of bow and stern

According to the last diagram of Figure12, the Semnan coefficient diagram mainly shows a downward trend with increasing the model number, but a maximum value occurs for model 3 that shows a good form of this model. It seems that model 3 with  $nf=1.35$  and  $na=4$  would be a good selection, because it has the maximum value of the Semnan coefficient and the minimum value of the resistance coefficient. Both show the best condition and ideal form. However, in real naval submarines, the form of model 3 can't be a good selection due to sharp shape bow and internal arrangement problems. The blunt, thick and bulky form is ideal and guarantees better arrangement of the bow and stern. From hydrodynamic form point of view, the more thin form is ideal. Thus, model 3 is the best form in this regard. According to this study, model 3 with  $nf=1.35$  and  $na=4$  has shown the best results. These diagrams show that an increase in the value of  $nf$  and  $na$  coefficients (more blunt and thick form) will cause a steep increase in the resistance coefficient values. The exact required values of  $nf$  and  $na$  depend on the other design parameters that stated above.

## 6. Bow form design

### 6.1. General Assumptions for the Models

In this section, 19 models are studied. There are three main assumptions:

**Assumptions 1.** For evaluating the hydrodynamic effects of bow, the length of the bow is unusually supposed large. It helps that the effects of the bow to be more visible.

**Assumptions 2.** For all models, the shapes of stern and middle part are assumed to be constant. The stern is conical and the middle part is cylindrical.

**Assumptions3.** For providing a more equal hydrodynamic condition, the total length and the lengths of bow, middle part and stern are assumed to be constant. The fineness ratio ( $L/D$ ) is constant as well, because the maximum diameter is constant. These assumptions provide an equal form resistance with except for the bow shape that varies in each model. Then, the effects of the bow shape can be studied. Therefore, the models have different volumes and wetted surface areas.

The main assumptions of all models are reported in Table 5.

**Table 5. Main assumptions of the models**

V	L	Lf	Lm	La	D	L/D	bow shape
[m/s]	[m]	[m]	[m]	[m]	[m]		
10	6	3	1	2	1	6	Different for each model

The analyses are conducted in two stages: Stage A) Based on the general shapes of the bow for understanding the basis and principles of submarine bow design. Stage B) Different bow shapes based on the Eqn. 2 for understanding the effect of different values of  $nf$  on the submarine bow design. This

equation is a well-known equation that covers a wide range of the bow forms. The specifications of the bow models regarding the stages A and B are reported in Table 6 and Table 7 respectively. In addition, for CFD modeling in relation to all models, the velocity is assumed constant and equal to 10 m/s. this value results Reynolds number more than 60 millions. This Reynolds is suitable for the turbulence modeling.

**Table 6. Model specifications of stage A**

bow shape profile	Aw	A0	volume
A1 ogive	12.77	0.785	2.58
A2 ogive- capped with circle	13.19	0.785	2.67
A3 conic	11.16	0.785	2.09
A4 conic caped with elliptic	14.41	0.785	3.03
A5 ship shape	13.85	0.785	2.49
A6 hemisphere	15.8	0.785	3.53
A7 elliptical	13.87	0.785	2.88
A8 DREA form (according to Eq.1)	15.19	0.785	3.33

The forms of these models are displayed in Figure13. In the model A1, bow is an ogive shape consists of an ogive slice of a circle so that to be tangent to the cylinder. Model A2 is an ogive shape that is capped by a circle. This shape is usual in small wet submarines. Model A3 has a conic bow that isn't usual in submarines but it is presented here to show why this type of bow isn't applicable in today's submarines. Model A4 has a conic bow that is capped by an elliptic so that both the elliptic and the conic are tangent to each other. Model A5 has a ship shape bow with a vertical sharp edge. This shape of bow is unusual in today's submarines because this bow shape is efficient for ships and free surface of water. This bow has minimum resistance in surfaced navigation but it has a large amount of resistance in submerged navigation. It was usual in old submarines because they had low battery storage and then, the most time of navigation was spent on the surface and only for attacking it was needed to go to submerged mode of navigation for a restricted time. Models A6 and A7 are hemispherical and elliptical bows respectively. Hemispherical bow isn't a common bow but the elliptical one is the most usual form of the bow. Most of the equations that stated above are similar to the elliptical bow. For example, in Eqn.2, for  $nf= 2$ , the bow shape profile is an elliptic form. Model A8 is designed according to Eqn. 8 for DREA submarine. The configurations of the models are shown in Figure13.

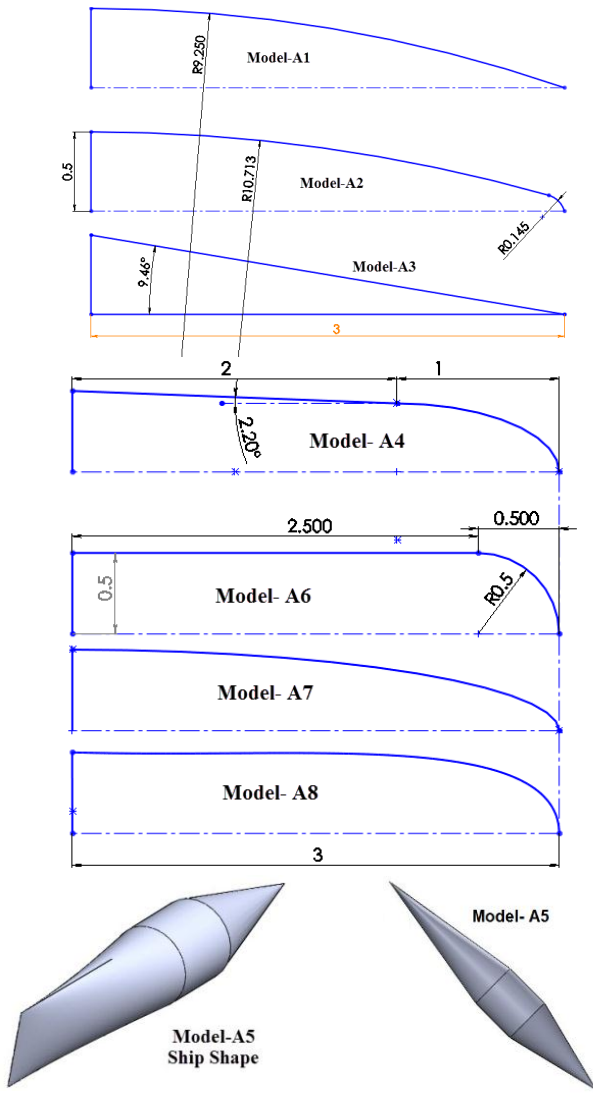
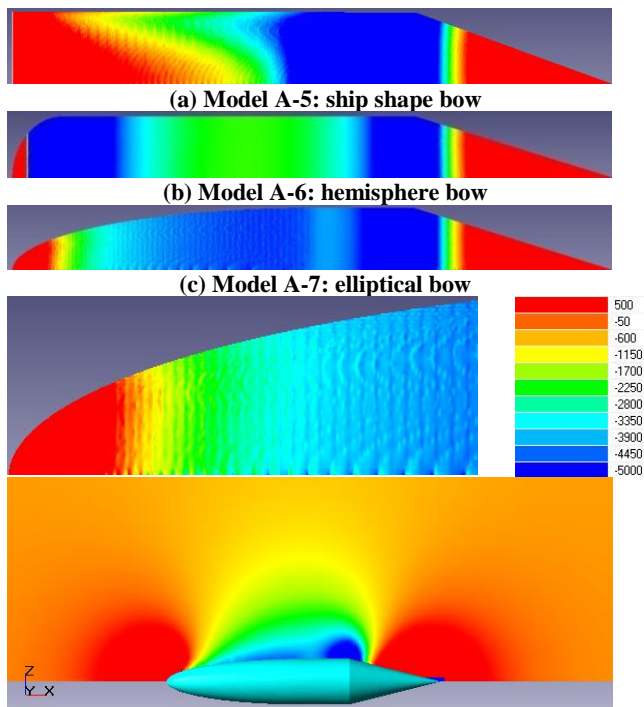


Figure 13. Bow configurations of the models (stage A)

The pressure distribution for several bow shapes is presented in Figure14.



(d) Contours of pressure and related values  
Figure 14. Pressure distribution over the body

The specifications of the bow models based on Eqn. 2 regarding the stage B are reported in Table 7.

Table 7. Model specifications of stage B based on Eqn.2

$n_f$		$A_w$	$A_0$	volume
B1	1	11.16	0.785	2.09
B2	1.15	11.79	0.785	2.26
B3	1.35	12.48	0.785	2.45
B4	1.5	12.9	0.785	2.58
B5	1.65	13.25	0.785	2.68
B6	1.75	13.45	0.785	2.75
B7	1.85	13.63	0.785	2.8
B8	2	13.87	0.785	2.88
B9	2.5	14.48	0.785	3.08
B10	3	14.87	0.785	3.21
B11	4	15.36	0.785	3.37
B12	5	15.64	0.785	3.46

The value of  $n_f$  can be varied between 1.8 and 4. For a better understanding of the effect of  $n_f$ , the range between 1 and 5 is considered as shown in Figure15. For  $n_f=2$ , the bow shape profile is an elliptic form and for  $n_f=1$ , the bow profile is a conical form. An increase in  $n_f$  will cause a corresponding increase in wetted surface area and enveloped volume as well. The configurations of the models are shown in Figure15.

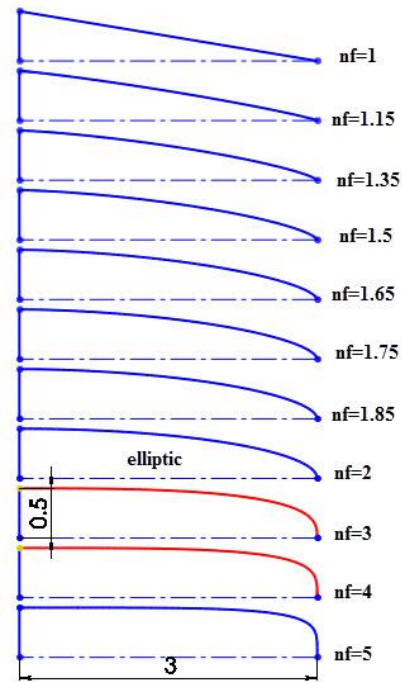


Figure 15. Configuration of bow part of models (stage B)

## 6.2. CFD Analysis of bow shape

The results of CFD analysis corresponding to stage A are reported in Table 8 and displayed in Figure16. In table 8,  $C_d$  is the resistance coefficient based on wetted area ( $A_w$ ). The resulting diagrams are shown in Figure16. The total resistances are shown inFigure16-a. According to this figure, under the assumption of constant length, the hemispherical bow has the most value and the conic bow has the least



**Table 8. Results of CFD analyses on different bow shapes (stage A)**

bow shape	Rt	Aw	Cd*1000	Semn.coef
ogive	1948	12.77	33.90	40.46
ogive-circle	2036	13.19	34.30	40.44
conic	1944	11.16	38.71	33.03
conic-elliptic	2416	14.41	37.26	38.84
ship shape	2488	13.85	39.92	33.95
hemisphere	3280	15.8	46.13	33.00
elliptical	2196	13.87	35.18	40.44
DREA	2624	15.19	38.39	38.90

value. The resistance coefficients based on wetted area are shown in Figure16-b. According to this figure, the hemisphere and ship shape bows have the most (worst) values, the ogive bow has the least (best) value and the elliptical and conic elliptical bows have the middle value of the resistance coefficients. Finally, Figure16-c represents the best criterion for judging between the bow shapes. This figure shows that the ogive shape has the most efficiency and the conic, hemisphere and ship shape bows have the least (worst) values. Now, it is possible to select a good bow shape. As shown in Figure 16, the bow shapes of conic, hemisphere and ship shape are the worse selections from resistance and volume point of view. Hemisphere bow shape has the most values of the resistance coefficient and the total resistance, while provides a good space for architecture but Figure16-c shows that it can't be a good selection. Conic bow shape results the minimum value of total resistance and the middle value of resistance coefficient but has the minimum volume (under the assumption of a constant length), then the conic bow shape can't be a good selection, as it is shown in Figure16-c with minimum efficiency.

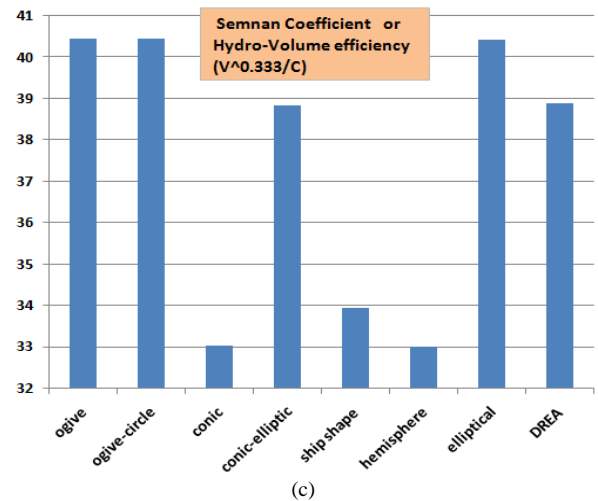
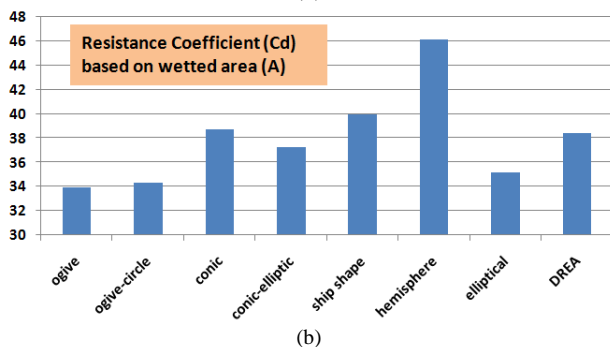
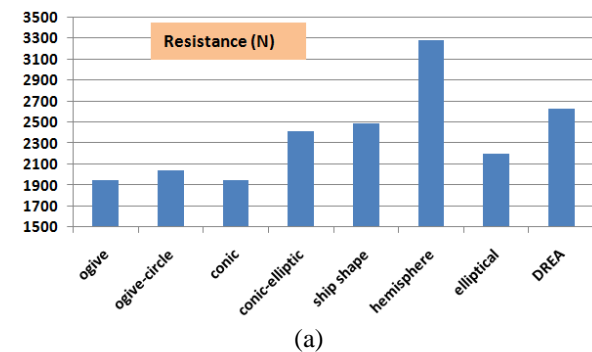


**Figure 16. Results of CFD analyses on different bow shapes (stage A)**

Ship shape bow has a high value of the resistance coefficient and the total resistance and a low value of volume. Therefore, it has a very low efficiency (according to Figure16-c) and is logical to reject the selection. Ogive and ogive capped with hemisphere have the minimum values of the resistance coefficient and the low values of the total resistance. Ogive bow seems to have a good condition from resistance point of view but isn't a good selection because it has a low value of volume. This bow has a steep frontal curvature that isn't a good configuration for arranging the sonar and torpedo tubes in the frontal part of real naval submarines. Thus, the ogive bow is rejected despite of the maximum value of the efficiency (according to Figure 16-c) and the minimum value of the resistance coefficient (according to Figure 16-b). Finally, three remaining bows (elliptical, conic elliptical and DREA form) can be discussed to be candidates for a good selection. DREA form has more total resistance and resistance coefficient compared to the other two bows, but instead it has better efficiency (according to Figure 16-c). Thus, it can be a good selection. In general, the elliptical bows are recommended.

The results of CFD analyses regarding stage "B" are reported in Table 9 and displayed in Figure17. The focus on this stage is on the Eqn.2 by the variation of the fullness parameter of the form ( $n_f$ ). This equation covers a wide variety of the bow profiles. Thus, the focus of this paper on stage "B" is related to it. As shown in Figure 17, the value of  $n_f$  can be varied between 1.8 and 4, but for better understanding of the effect of  $n_f$  the considered range has been selected between 1 and 5. An increase in  $n_f$  will cause a corresponding increase in wetted surface area and enveloped volume as well. In this section, the range of  $n_f$  between 1.35 and 2 is more precisely studied because this range has some extreme points. When  $n_f$  is larger than 2, the gradient is approximately linear. The values of  $n_f$  which are less than 1.35 aren't common practice in naval submarines, as discussed in

stage A. An overview on the results shows that, in this range,  $n_f=1.85$  has the maximum total resistance and resistance coefficient and the minimum efficiency coefficient that means the worst results. The total resistance diagram shows that  $n_f=1.15$  has the minimum value and  $n_f=1.85$  has the most value. Bow shape based on  $n_f=1.15$  is a sharp bow that isn't suitable from architecture point of view.

According to Figure17-b, the resistance coefficient has the minimum (best) value at  $n_f=1.35$  and the maximum (worst) value at  $n_f=1.85$ . The most important parameter that can be used for judging between them is shown in Figure17-c. This diagram shows the presence of local maximum points around  $n_f=1.5$  and  $n_f=2$ . This means the presence of good selections as well, especially at  $n_f=1.5$  that the maximum hydro-volume efficiency is exist (from Semnan coefficient point of view). Figure 17-c shows the presence of a local minimum point between  $n_f=1.75$  and  $n_f=1.85$  which must be avoided in design process.

**Table 9. Results of CFD analyses on different bow shapes (stage B)**

$n_f$	Rt[N]	Aw [m <sup>2</sup> ]	Volume [m <sup>3</sup> ]	Cd*1000	$V^{0.33} / (Cd*10)$
1	1944	11.16	2.09	3.484	36.69
1.15	1820	11.79	2.26	3.087	42.49
1.35	1876	12.48	2.45	3.006	44.83
1.5	1952	12.9	2.58	3.026	45.31
1.65	2060	13.25	2.68	3.109	44.66
1.75	2200	13.45	2.75	3.271	42.81
1.85	2264	13.63	2.8	3.322	42.41
2	2196	13.87	2.88	3.167	44.92
2.5	2388	14.48	3.08	3.298	44.10
3	2724	14.87	3.21	3.664	40.25
4	3052	15.36	3.37	3.974	37.71
5	3368	15.64	3.46	4.307	35.10

According to these diagrams, some formulas can be fitted to them. The formula for relation between resistance coefficient (Cd) and  $n_f$  is:

For  $1.15 < n_f < 2$ :

$$C_d = (-11.85 \cdot n_f^4 + 70.31 \cdot n_f^3 - 153.73 \cdot n_f^2 + 146.62 \cdot n_f - 48.48) \cdot 10^{-3} \quad (10)$$

This section has shown that: 1) "Semnan Coefficient" can be presented as an important parameter in submarine shape design that counts both parameters: resistance coefficient and volume. It can be named "hydro-volume efficiency". 2) Conic bow and ship shape bow aren't good for selection because of high values of resistance coefficient and very low values of hydro-volume efficiency. 3) Simple hemispherical bow isn't a good selection in the design process because of the high value of resistance coefficient and the least value of hydro-volume efficiency. This form is not recommended at all. 4) Ogive bow shape has a good result in resistance coefficient and hydro-volume efficiency but this shape isn't a common practice in

real naval submarines because of many difficulties in the internal arrangements of the bow. 5) Elliptical bow and the other shapes similar to that have the best acceptable results in resistance coefficient and hydro-volume efficiency. This shape of bow is highly recommended.

6) The coefficients around  $n_f=1.75 \sim 1.85$  may have the worse results but the coefficients around  $n_f=1.5$  and 2 are good selections for design, especially in  $n_f=1.5$  that has maximum hydro-volume efficiency.

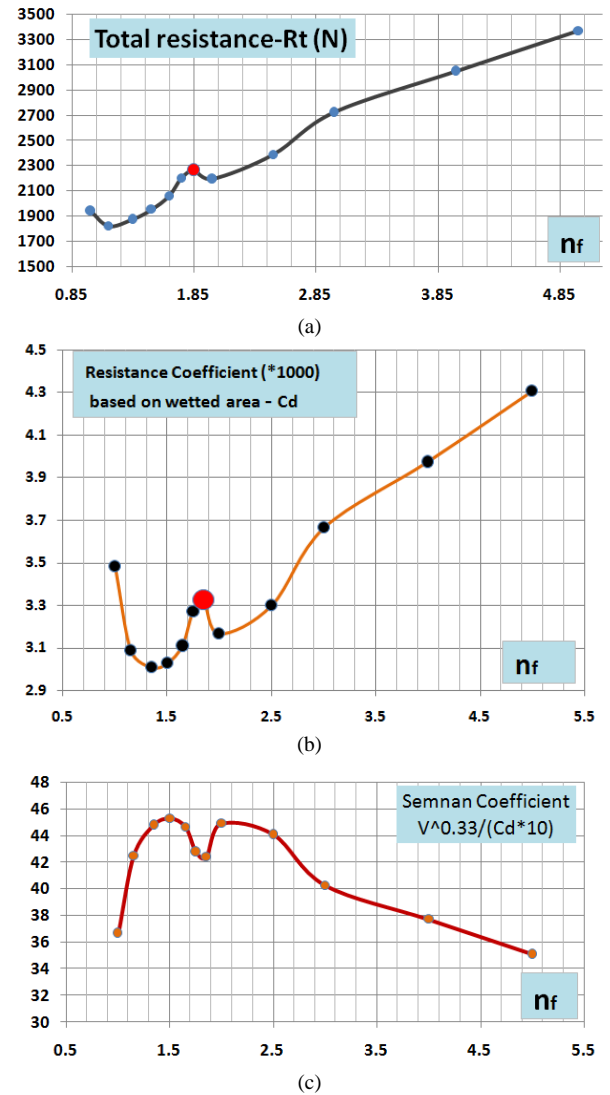


**Figure 17. Results of CFD analyses on different bow shapes (stage B)**

## 7. Stern Form Design

### 7.1. Equations of Stern Form

#### 7.1.1. Parabolic

This stern shape isn't the blunt shape. The parabolic series shape is generated by rotating a segment of a parabola around an axis. This construction is similar to that of the tangent ogive, except that a parabola is the defined shape rather than a circle. This construction, according to Figure18-a, produces a stern shape with a sharp tip, Just as it does on an ogive case.

For  $0 \leq K' \leq 1$ :

$$y = R \left( \frac{2\left(\frac{x}{L}\right) - K' \left(\frac{x}{L}\right)^2}{2 - K'} \right) \quad (11)$$

$K'$  can be set anywhere between 0 and 1, but the values most commonly used for stern shapes are as follows:  $K'=0$  for a cone,  $K'=0.5$  for a 1/2 parabola,  $K'=0.75$  for a 3/4 parabola and  $K'=1$  for a full parabola. For the case of full Parabola ( $K'=1$ ) the shape is tangent to the body at its base and the base is on the axis of the parabola. It is important from view point of the reduction of resistance. Values of " $K'$ " less than one, result in a slimmer shape, whose appearance is similar to that of the secant ogive. The shape is no longer tangent at the base, and the base is parallel to, but offset from, the axis of the parabola.

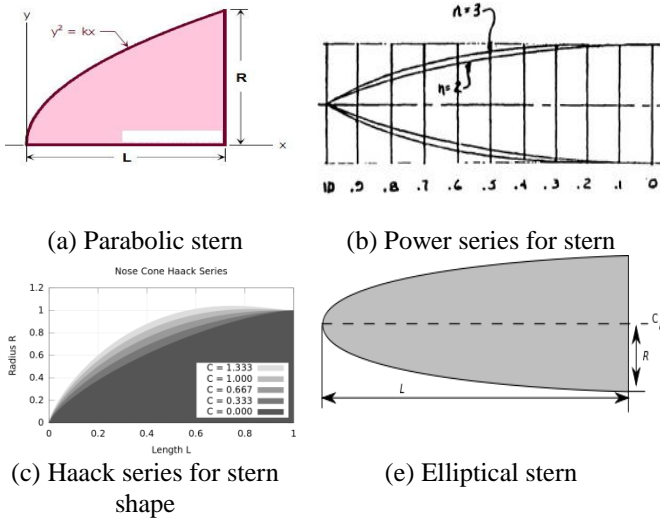


Figure 18. Several shapes of stern [26,27]

### 7.1.2. Power series

According to Eqn.3 and Figure18-b, the power series includes the shape commonly referred to as a "parabolic" stern, but the shape correctly known as a parabolic stern is a member of the parabolic series (described above). The power series shape is characterized by its tip (usually blunt tip) and the fact that its base isn't tangent to the body tube. There is always a discontinuity at the joint between stern and body that looks distinctly non-hydrodynamic. The shape can be modified at the base to smooth out this discontinuity. Both a flat-faced cylinder and a cone are shapes that are members of the power series. The after body is generated by revolving a line around an axis and is described by Eqn.3.

The factor " $n_a$ " controls the bluntness of the shape. Then for " $n_a$ ", it can be said:  $n_a=1$  for a cone,  $n_a=2$  for a elliptic,  $n_a=0$  for a cylinder.

### 7.1.3. Haack series

despite of all the stern shapes above, the Haack Series shapes are not constructed from geometric figures. The shapes are instead mathematically derived for minimizing resistance. While the series is a continuous set of shapes determined by the value of  $C$  in the equations below, two values of  $C$  have

particular significance: when  $C=0$ , the notation LD signifies minimum drag for the given length and diameter, and when  $C=1/3$ , LV indicates minimum resistance for a given length and volume. The Haack series shapes are not perfectly tangent to the body at their base, except for a case where  $C=2/3$ . However, the discontinuity is usually so slight as to be imperceptible. For  $C > 2/3$ , Haack stern bulges to a maximum diameter greater than the base diameter. Haack nose tips do not come to a sharp point, but are slightly rounded (Figure18-c).

$$\theta = \arccos \left( 1 - \frac{2x}{L} \right) \quad y = \frac{R}{\sqrt{\pi}} \sqrt{\theta - \frac{\sin(2\theta)}{2} + C \sin^3 \theta} \quad (12)$$

Where:  $C = 1/3$  for LV-Haack and  $C = 0$  for LD-Haack.

### 7.1.4. Von Karman

The minimum drag, under the assumption of constant length and diameter, is offered by the Haack series. LD-Haack is commonly referred to as the Von Karman or the Von Karman Ogive.

### 7.1.5. Elliptical

According to Figure18-e, this shape of the stern is an ellipse, with the major axis being the centerline and the minor axis being the base of the stern. A body that is generated by a rotation of a full ellipse about its major axis is called a prolate spheroid, so an elliptical stern shape would properly be known as a prolate hemispheric. This is not a shape normally found in the usual submarines. If  $R$  is equal to  $L$ , then the shape will be a hemisphere.

$$y = R \sqrt{1 - \frac{x^2}{L^2}} \quad (13)$$

## 7.2. General Assumptions for the Models

There are three main assumptions:

**Assumptions 1.** For evaluating the hydrodynamic effects of stern, the length of the stern is unusually supposed large. It helps that the effects of the stern to be more visible.

**Assumptions 2.** For all models, the shapes of bow and middle part are assumed to be constant. The bow is elliptical and the middle part is cylindrical.

**Assumptions3.** For providing a more equal hydrodynamic condition, the total length and the lengths of bow, middle part and stern are assumed to be constant. The fineness ratio ( $L/D$ ) is constant as well, because the maximum diameter is constant. The assumed constant parameters provide an equal form resistance with except for the stern shape that varies in each model. Then, the effects of the stern shape can be studied. Therefore, the models have different volumes



and wetted surface areas. The specifications of all considered models are reported in Table 10.

**Table 10: Main assumptions of the models**

v [m/s]	Lt [m]	Lf [m]	Lm [m]	La [m]	D [m]	Lt/D	A0 [m <sup>2</sup> ]
10	8	2	1	5	1	8	3.14

The specifications of all 19 models are presented in Figure 19 and reported in Table 11.

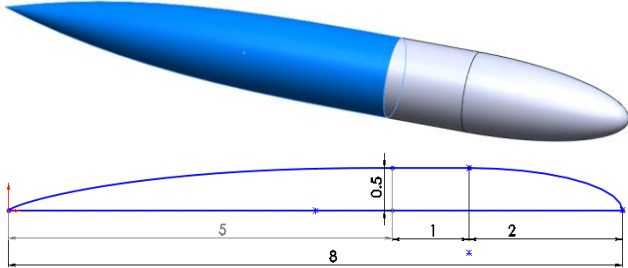


**Figure 19. General configuration of the models**

For all models, the volume of bow and cylinder is constant and equal to 1.83 cubic meters but the total volumes are different. In addition, for CFD modeling in relation to all models, the velocity is assumed constant and equal to 10 m/s.

**Table 11. specifications of 19 models**

MODEL	specification of stern	Aw[m <sup>2</sup> ]	V[m <sup>3</sup> ]
Model 1-1	parabolic with k'=0.3	16.55	3.26
Model 1-2	parabolic with k'=0.5	16.96	3.37
Model 1-3	parabolic with k'=0.6	17.21	3.45
Model 1-4	parabolic with k'=0.75	17.66	3.58
Model 1-5	parabolic with k'=0.85	18.02	3.7
Model 1-6	parabolic with k'=1	18.71	3.93
Model 2-1	power series - n=1.5	17.66	3.6
Model 2-2	power series - n=1.65	18.01	3.71
Model 2-3	power series - n=1.85	18.43	3.84
Model 2-4	power series - n=2 (Elliptic)	18.71	3.93
Model 2-5	power series - n=3	20.03	4.36
Model 2-6	power series - n=4	20.83	4.63
Model 2-7	power series - n=5	21.36	4.81
Model 2-8	power series - n=6	21.75	4.94
Model 2-9	power series - n=8	22.27	5.12
Model 3-1	Haack series with c=0	18.47	3.8
Model 3-2	Haack series with c=0.15	18.83	3.91
Model 3-3	Haack series with c=0.333	19.24	4.04
Model 3-4	Haack series with c=0.666	19.95	4.29

The configurations of all models including Parabolic models (models 1-1 to 1-6), power series models (models 2-1 to 2-9) and Haack series models (models 3-1 to 3-4) are displayed in Figure 20, Figure 21 and Figure 22 respectively.

### 7.3. CFD Analysis on Stern Shape

Pressure contours around the body are shown in Figure 23 for sample.

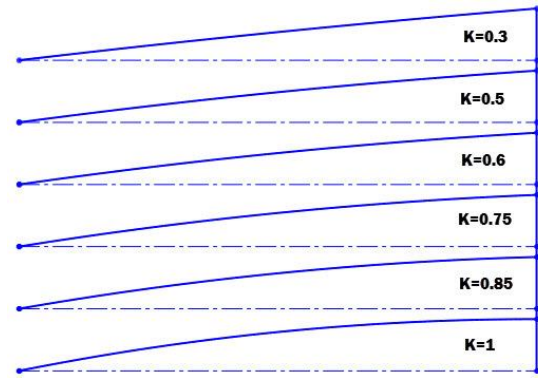


**Figure 20: Configurations of parabolic models**

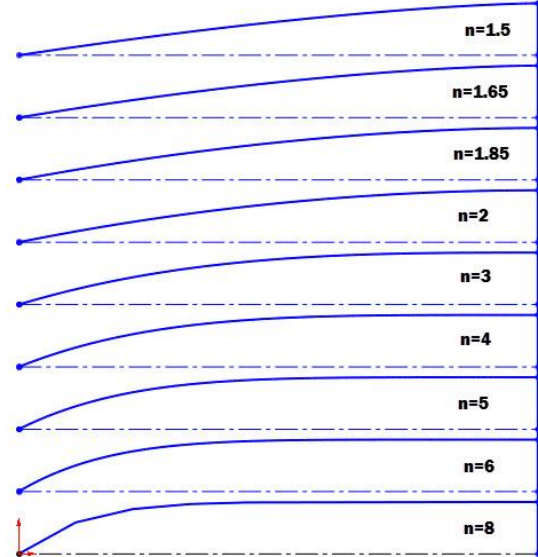


**Figure 21. Configurations of power series models**

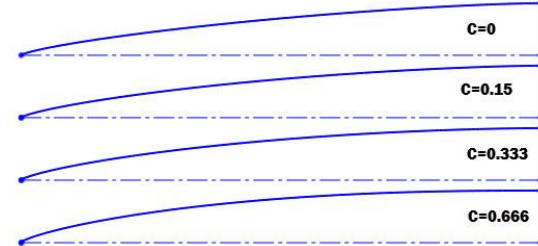


**Figure 22. Configurations of Haack series models**

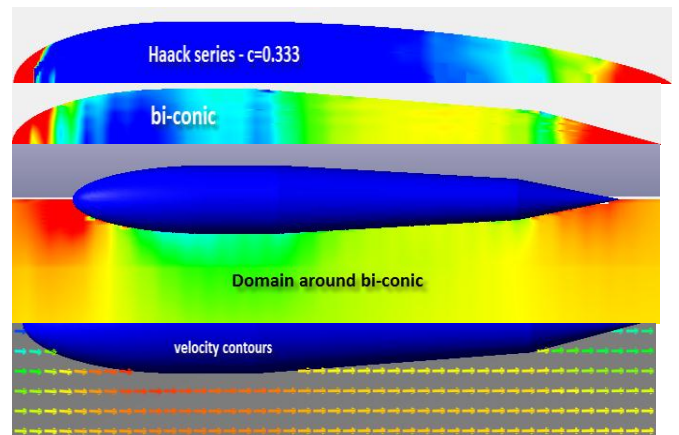


**Figure 23. pressure contour around the body**

The diagrams of the total resistance, resistance coefficient and Semnan coefficients corresponding to the Parabolic, power series and Haack series sterns are shown in Figs. 24, 23 and 24, respectively. In the Parabolic stern form, according to Figure 24, the total



resistance increases and the resistance coefficient decreases with increasing of  $K'$ . It means that, under the assumption of constant length, the lesser value of  $K'$  is better and, under the assumption of constant wetted surface area, the more value of  $K'$  is better. For having a better criteria, from view point of naval architecture design, "Semnan" coefficient needs to be more for providing simultaneously both the lesser value of resistance coefficient and the more value of enveloped volume. Here, the more value of  $K'$  means the more value of Semnan coefficient and the better condition as well. The equation of resistance coefficient is stated as follows:

$$C_t = -1.572(K') + 30.35 \quad (14)$$

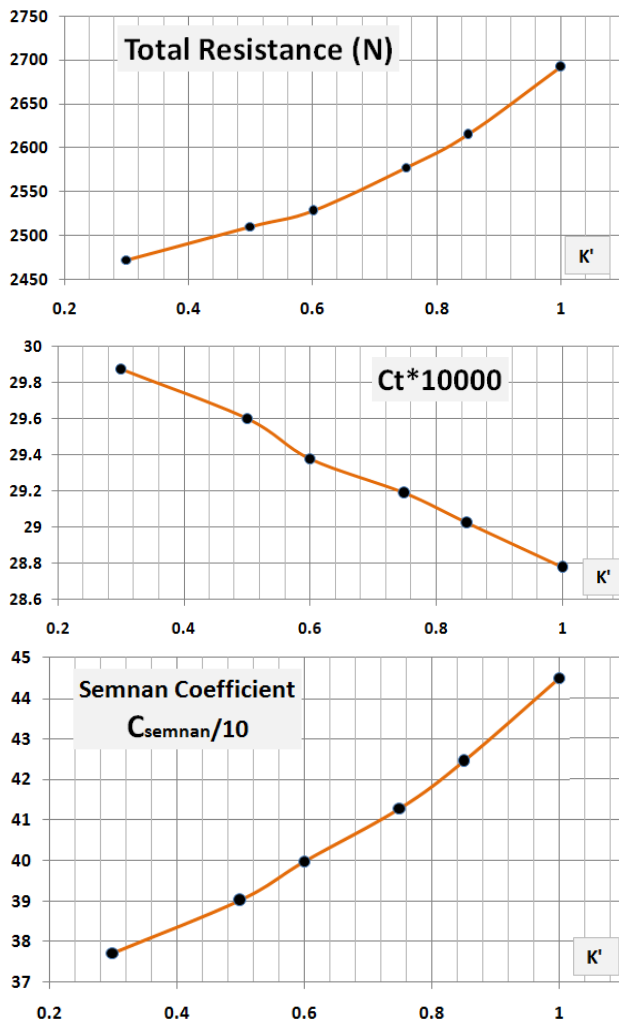


Figure 24. Variation of the total resistance, resistance coefficient and Semnan coefficient with  $K'$  for Parabolic stern

In the Power Series stern form, according to Figure 25, the total resistance increases with increasing of  $n_a$ . The resistance coefficient diagram has two minimum points: a local minimum at  $n_a=1.85$  and a global minimum at  $n_a=4$ . It means that, under the assumption of constant length, the lesser value of  $n_a$  is better but, under the assumption of constant wetted surface area with regard to the resistance coefficient, the values of  $n_a$  around 4 are better. For this form, the Semnan coefficient has a maximum value around

$n_a=5.6$  that shows the best selection regarding design process. In this regard, the equation of resistance coefficient for  $2 < n_a < 8$  is as follows:

$$C_t = -0.01(n_a)^3 + 0.33(n_a)^2 - 2.11(n_a) + 33.03 \quad (15)$$

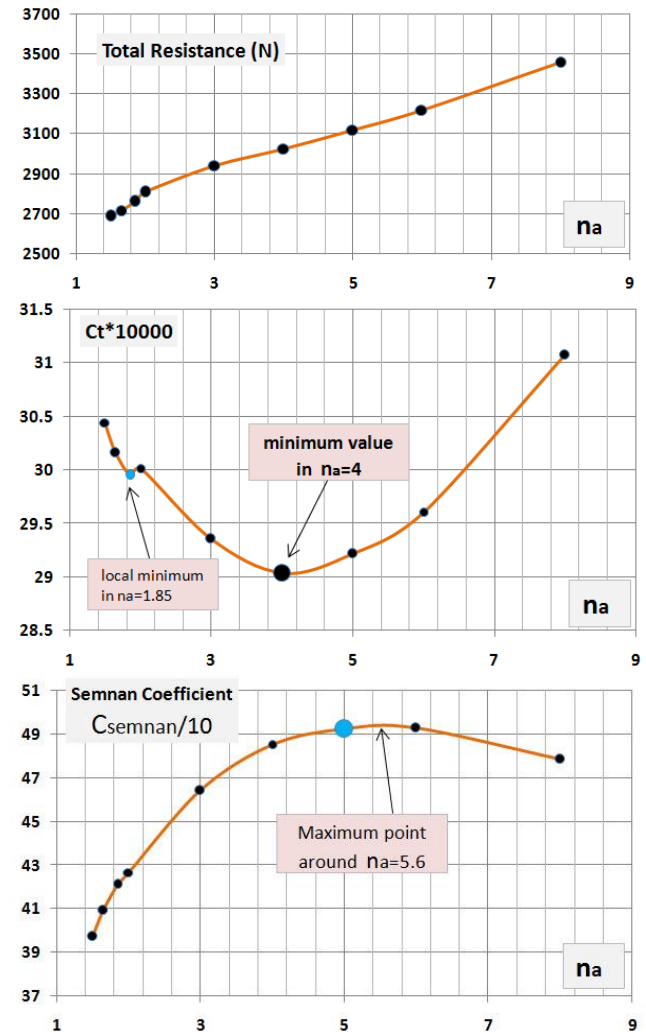


Figure 25. Variation of the total resistance, resistance coefficient and Semnan coefficient with  $n_a$  for Power series stern

In the Haack Series stern form, according to Figure 26, the total resistance increases with increasing of  $C$ . This variation is exactly linear. It means that, under the assumption of constant length, the lesser value of  $C$  is better but, under the assumption of constant wetted surface area with regard to the resistance coefficient, the values of  $C$  around 0.3 are better. For this form, the Semnan coefficient increases with increasing of " $C$ ". In this regard, the equation of resistance coefficient is as follows:

$$C_t = 30.9839 + 0.2066 \cos(9.176C + 0.1161) \quad (16)$$

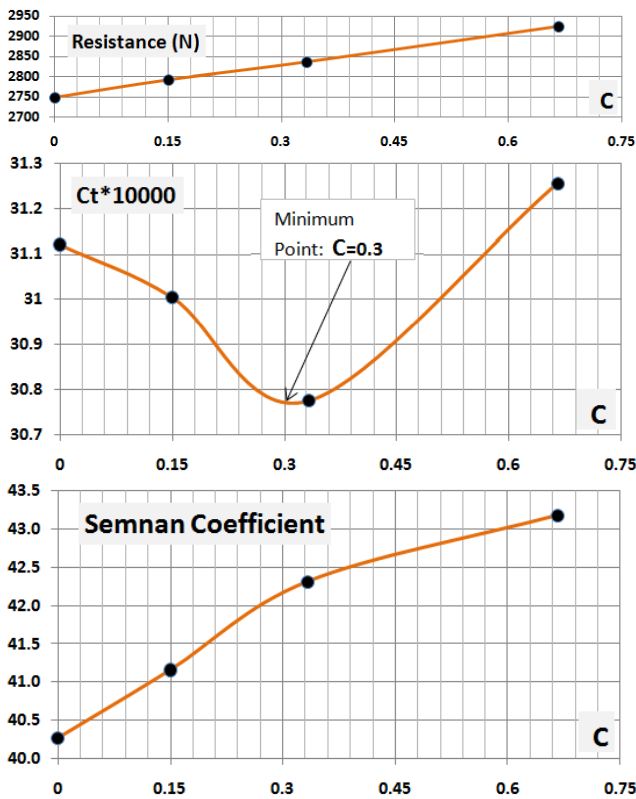


Figure 26. Variation of the total resistance, resistance coefficient and Semnan coefficient with C for Haack series stern

In conclusion, the results of this study can be stated as follows: 1) In the Parabolic stern form, under the assumption of constant length, the value of  $K'=0.3$  is a good selection but, under the assumption of constant wetted surface area, the stern form with  $K'=1$  is the best design, because the maximum value of Semnan coefficient is achieved in this value. 2) In the Power Series stern form, under the assumption of constant wetted surface area, there are two minimum points around  $n_a=1.85$  and 4 which offer good selections but, under the assumption of constant length, the stern form with  $n_a=5.6$  is the best design, because the maximum value of Semnan coefficient is achieved in this value. 3) In the Haack Series stern form, under the assumption of constant wetted surface area, the value of  $C=0.3$  is a good selection because the minimum resistance coefficient is achieved in this value. Under the assumption of constant length, the stern form with  $C=0.66$  is the best design because the more values of "C" is equal to the more values of Semnan coefficient. 4) A comparison between the three types of stern shapes, under the assumption of constant wetted surface area, indicates that the Haack series stern form has the worse result by the most value of resistance coefficient. The power series stern form, under the assumption of constant length, has the worse result by the most value of resistance. For providing more volume with the lesser resistance coefficient, based on the maximum value of Semnan coefficient, the power series stern form has the most value and offers the best result. 5) Finally, the best advice of this paper for the stern form of submarine based on the diagrams of

Semnan coefficients is "Power series" in the range of 4 to 6 for  $n_a$ .

## 8. Optimum L/D for Submarine Shape

### 8.1. General Assumptions for the Models

In this section, the fineness ratio (L/D) is only needed to be studied. Hence, the base model that is considered in this section is an axis-symmetric body similar to torpedo, without any appendages. The bow is elliptical and stern is conical. There are two main assumptions:

#### Assumptions 1.

For evaluating the hydrodynamic effects of L/D, the total volume of shape is considered to be constant and only L/D ratios are changed. In this section, eleven models are considered. In all models, the total volume is equal to 5.89 cubic meters. Base model is L/D=10, and other models are changed so that L/D varies with constant volume and because of that, the length amount has two decimal numbers. The 3D forms and volume properties are modeled in Solid Works by try and error method.

#### Assumptions 2.

For providing more equal hydrodynamic conditions, the bow and stern length are proportioned to the diameter. This constant proportion provides equal form resistance with except L/D and then the effects of L/D can be studied. In all models, the bow length is equal to 1.5D and the stern length is 3D.

Various values of the L/D ratio corresponding to these 11 models are as follows: 3.98, 5.48, 7.18, 7.98, 8.45, 10, 10.71, 11.53, 13.13, 13.88 and 15.15. In addition, for CFD modeling in relation to all models, velocity is assumed constant and equal to 2 m/s. Some of models are shown in Figure27.

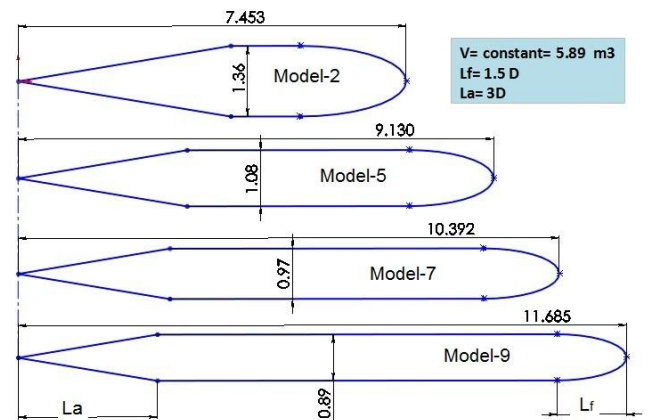


Figure 27. Some of models with different L/D but constant volume

### 8.2. CFD Analysis

Some studies about the hydrodynamic effects of fineness ration(L/D) are performed by CFD method [12]. The pressure resistance diagram shows a downward trend with increasing L/D. It means that an increase in L/D will cause a corresponding decrease in the pressure resistance. The higher L/D values cause a

more stream-lined shape that results the more time for matching the fluid flow with the body. The frictional resistance diagram shows an upward trend with increasing  $L/D$ . It means that an increase in  $L/D$  will cause a corresponding increase in the frictional resistance. The higher  $L/D$  values cause a more wetted surface area. Therefore, an increase in  $L/D$  will lead to an increase in the frictional resistance and a decrease in the pressure resistance.

This fact shows the opposite trends of the resistance coefficients (pressure and frictional). The total resistance is equal to the summation of these two resistances; then an optimum  $L/D$  or optimum range for  $L/D$  should be available. Figure 28 shows the optimum range of  $L/D$  for cylindrical middle body submarine. According to this diagram, the optimum range of  $L/D$  for cylindrical middle body submarines is between 7 and 10. In several scientific references such as Ref. [3], the optimum hydrodynamic value of  $L/D$  for tear drop shape is 7.

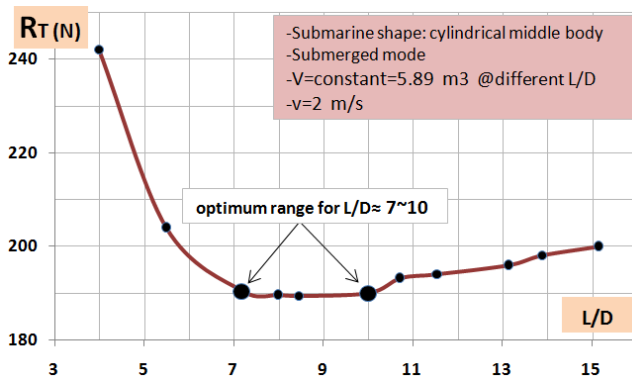


Figure 28. Optimum range of  $L/D$  for cylindrical middle body submarine

The main achievement of this section is the suggestion of fineness ratio ( $L/D$ ) between 7 and 10 as the optimum range for cylindrical middle body submarine. Formerly, this range was suggested between 6 and 7 for tear drop shapes. Other achievements of this section are as follows: 1) Pressure resistance decreases with increasing  $L/D$  but before the optimum range this decrease is steeper. 2) Frictional resistance increases with increasing  $L/D$  but this variation is mild entirely. 3) All resistance coefficients (pressure, frictional and total) decrease versus  $L/D$ . Here it should be notified that resistance trend is different from the resistance coefficient. 4) Wetted surface area increases versus  $L/D$  that causes an increase in frictional resistance despite decrease in the resistance coefficient.

Schematic representation of the resistance variation versus fineness ratio  $L/D$  is shown in Figure 29.

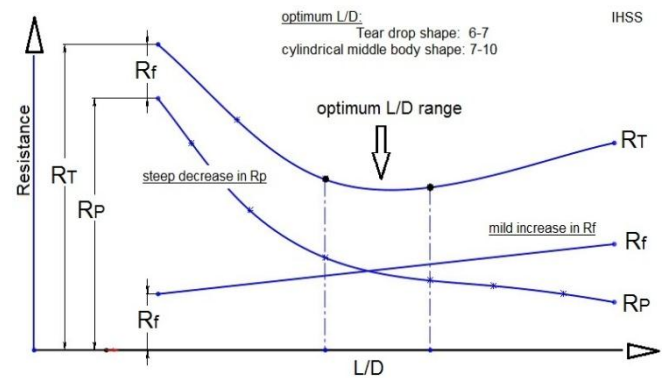


Figure 29. Schematic representation of the resistance variation versus fineness ratio  $L/D$

## 9. Conclusion

In this paper, various design factors such as bow and stern form, general shapes and fineness ratio ( $L/D$ ) affecting the submarine bare hull form design are considered. The major conclusions of each section are presented at the end of that section. The comparison of simulation and experimental results shows that the results of Flow Vision software are reliable in CFD modeling. "Semnan Coefficient" as an important parameter in the process of submarine form design is introduced in this paper from naval architecture point of view.

## 10. Nomenclature

$C_s$	Surface coefficient
$C_p$	Prismatic coefficient
$C_f$	Friction resistance coefficient
$C_R$	Residual resistance
$C_t$	Total resistance coefficient
CFD	Computational Fluid Dynamics
$D$	maximum diameter of the outer hull [m]
IHSS	Iranian Hydrodynamic Series of Submarines
$L$	overall length of hull [m]
$L_a$	Length of aft (stern) [m]
$L_f$	Length of forward part (bow) [m]
$n_f$	Coefficient of fore (bow) part of bare hull
$n_a$	Coefficient of aft (stern) part of bare hull
$R$	maximum radius of the outer hull [m]
$X'$	$= \text{Resistance} / 0.5 \rho U^2 L^2$ [m]
$x_a$	X from stern [m]
$x_f$	X from bow [m]
$y_a$	Y from axis in bow [m]
$y_f$	Y from axis in stern [m]

\* Other parameters are shown on the figures or described inside the text.

## 11. References

- 1- Joubert, P.N., (2004), *Some aspects of submarine design: part 1: Hydrodynamics*, Australian Department of Defence.
- 2- Joubert, P.N., (2004), *Some aspects of submarine design: part 2: Shape of a Submarine 2026*, Australian Department of Defence.
- 3- Burcher, R., Rydill, L.J., (1998), *Concept in submarine design*, The press syndicate of the University of Cambridge, Cambridge university press, p. 295.

- 4- Yuri, N.K., Oleg, A.K., (2001), *Theory of Submarine Design*, Saint Petersburg State Maritime Technical University, Russia, p.185-221.
- 5- Moonesun, M., Javadi, M., Charmdooz, P., Korol, U.M., (2013), *Evaluation of submarine model test in towing tank and comparison with CFD and experimental formulas for fully submerged resistance*, Indian Journal of Geo-Marine Science, vol.42(8), p.1049-1056.
- 6- Moonesun, M., (2014), *Introduction of Iranian Hydrodynamic Series of Submarines (IHSS)*, Journal of Taiwan Society of Naval Architects and Marine Engineers, Vol.33, No.3, p.155-162.
- 7- Moonesun, M., Korol, Y.M., (2014), *Concepts in submarine shape design*, The 16th Marine Industries Conference (MIC2014), Bandar Abbas, Iran.
- 8- Moonesun, M., Korol, Y.M., Brazhko, A., (2015), *CFD analysis on the equations of submarine stern shape*, Journal of Taiwan Society of Naval Architects and Marine Engineers, Vol.34, No.1, p.21-32,.
- 9- Moonesun, M., Korol, Y.M., Tahvildarzade, D., *Optimum L/D for Submarine Shape*, Indian Journal of Geo-Marine Science (In press).
- 10- Moonesun, M., Korol, Y.M., Tahvildarzade, D., Javadi, M., (2014), *Practical solution for underwater hydrodynamic model test of submarine*, Journal of the Korean Society of Marine Engineering, Vol.38, No.10, p.1217-1224.
- 11- Iranian Defense Standard (IDS- 857), (2011), *Hydrodynamics of Medium Size Submarines*.
- 12- Praveen, P.C., Krishnankutty, P., (2013), *study on the effect of body length on hydrodynamic performance of an axi-symmetric underwater vehicle*, Indian Journal of Geo-Marine Science, vol.42(8), p.1013-1022.
- 13- Suman, K.S., Nageswara, R.D., Das, H.N., Bhanu, G. K., (2010), *Hydrodynamic Performance Evaluation of an Ellipsoidal Nose for High Speed Underwater Vehicle*, Jordan Journal of Mechanical and Industrial Engineering (JJMIE), Vol.4, No.5, p.641-652.
- 14- Mackay, M., (2003), *The Standard Submarine Model: A Survey of Static Hydrodynamic Experiments and Semiempirical Predictions*, Defence R&D Canada, p.30
- 15- Baker, C., (2004), *Estimating Drag Forces on Submarine Hulls*, Defence R&D Canada, p.131.
- 16- Alemayehu, D., Boyle, R.B., Eaton, E., Lynch, T., Stepanchick, J., Yon, R., (2005), *Guided Missile Submarine SSG(X), SSG(X) Variant 2-44*, Ocean Engineering Design Project, AOE 4065/4066, Virginia Tech Team 3 ,p.11-12.
- 17- Minnick, Lisa., (2006), *A Parametric Model for Predicting Submarine Dynamic Stability in Early Stage Design*, Virginia Polytechnic Institute and State University, , p.52-53.
- 18- Grant, B.T., (1994), *A design tool for the evaluation of atmosphere independent propulsion in submarines*, Massachusetts Institute of Technology, p.191-193.
- 19- Jackson, H.A., CAPT, P.E., (1983), *Submarine Parametrics*, Royal institute of naval architects international symposium on naval submarines, London, England.
- 20- Stenars, J.K., (1988), *Comparative naval architecture of modern foreign submarines*, Massachusetts Institute, p.91.
- 21- Prestero, T., (1994), *Verification of a Six-Degree of Freedom Simulation Model for the REMUS Autonomous Underwater Vehicle*, University of California at Davis, p.14-15.
- 22- Myring, D.F., (1976), *A Theoretical study of body drag in subcritical axisymmetric flow*.
- 23- Hoerner, S.F., (1965), *Fluid Dynamic Drag*.
- 24- Greiner, L., (1968), *Underwater missile propulsion : a selection of authoritative technical and descriptive papers*.
- 25- Denpol, E.V., (1976), *An estimation of the normal force and the pitching moment of 'Teardrop' underwater vehicle*.
- 26- Groves, N.C., Haung, T.T., Chang, M.S., (1989), *Geometric Characteristics of DARPA SUBOFF model*, David Taylor Research Centre.
- 27- Roddy, R., (1990), *Investigation of the stability and control characteristics of several configurations of the DARPA SUBOFF model (DTRC Model 5470) from captive-model experiment*, Report No. DTRC/SHD-1298-08.
- 28- Jerome, S.P., Raymond, E.G., Fabio, R.G., (1974), *Shaping of Axisymmetric Bodies for Minimum Drag in Incompressible Flow*, Journal of Hydronautics, Vol.8, No.3, p.100-108.
- 29- Brenden, M., (2010), *Design and Development of UUV*, University of New South Wales, Australian Defence Force Academy, School of Engineering and Information Technology Canberra, Thesis Report.
- 30- Volker, B., Alvarez, A., (2007), *Hull Shape Design of a Snorkeling Vehicle*, Institute Mediterrani d'Estudis Avancats (IMEDEA).
- 31- Moonesun, M., Korol, Y.M., Tahvildarzade, D., Javadi, M., *CFD analysis on the equations of submarine bow shape*, Journal of the Korean Society of Marine Engineering (In press).
- 32- Behzad, M., Rad, M., Taghipour, R., Mousavi, S.M., Sadat, S.H., Hosseini., (2004), *Parametric study of hull operability in waves for a tourist submarine*, International Journal of Maritime Technology.